SUPPORTING INFORMATION

The effect of halogen bonding on protonated hexacyanoferrate networks in hexacyanoferrates of halogenopyridines

Nikola Jakupec, Luka Fotović and Vladimir Stilinović

Department of Chemistry, Faculty of Science, University of Zagreb, Horvatovac 102a, HR-10000 Zagreb, Croatia

Email: vstilinovic@chem.pmf.hr
Fax: +385 1 4606 341
Tel: +385 1 4606 371

Table of Contents

Table S1. Crystal data and refinement details for the prepared salts.

	I	II	III	IV
Molecular formula	$C_{26}H_{26}Cl_2FeN_{10}O_2$	$C_{58}H_{44}Br_8Fe_3N_{26}$	$C_{16}H_{12}FeI_2N_8$	$C_{34}H_{32}Cl_4Fe_2N_{16}O_2$
M_r	574.35	1911.90	626.00	950.20
Crystal system	monoclinic	monoclinic	monoclinic	triclinic
Space group	$P\,2_1/n$	$P\,2_1/n$	$P\,2_1/n$	$P\,{-}1$
Crystal data:				
a / Å	8.7562(6)	19.931(2)	8.3887(4)	8.1771(9)
b / Å	13.1732(10)	12.6943(14)	9.6390(5)	11.2544(12)
c / Å	12.6457(7)	30.341(3)	13.2734(7)	12.1692(15)
α / °	90	90	90	91.426(9)
β / °	95.040(6)	93.819(8)	99.110(5)	108.865(10)
γ / °	90	90	90	90.318(9)
V / Å^3	1453.01	7659.53	1059.73	1059.32
Z	2	4	2	1
D_{calc} / g cm^{-3}	1.46	1.66	1.96	1.49
$\lambda(MoK_\alpha)$ / Å	0.71073	0.71073	0.71073	0.71073
T / K	295	295	295	295
Crystal size / mm^3	0.20 x 0.18 x 0.16	0.12 x 0.09 x 0.06	0.28 x 0.20 x 0.12	0.32 x 0.22 x 0.12
μ / mm^{-1}	0.746	4.787	3.642	0.989
$F(000)$	656	3728	592	484
Refl. collected/unique	5298 / 2531	13322 / 7459	10615 / 2306	8386 / 4211
Data/restraints/ parameters	174	402	132	278
$\Delta\rho_{max}$, $\Delta\rho_{min}$ / e Å^{-3}	0.71; −0.99	1.64; −1.63	1.19; −1.21	0.52; −0.59
$R[F^2 > 4\sigma(F^2)]$	0.066	0.1075	0.0392	0.0433
$wR(F^2)$	0.144	0.281	0.093	0.074
Goodness-of-fit, S	0.845	1.018	1.046	1.020

Table S1. Continued.

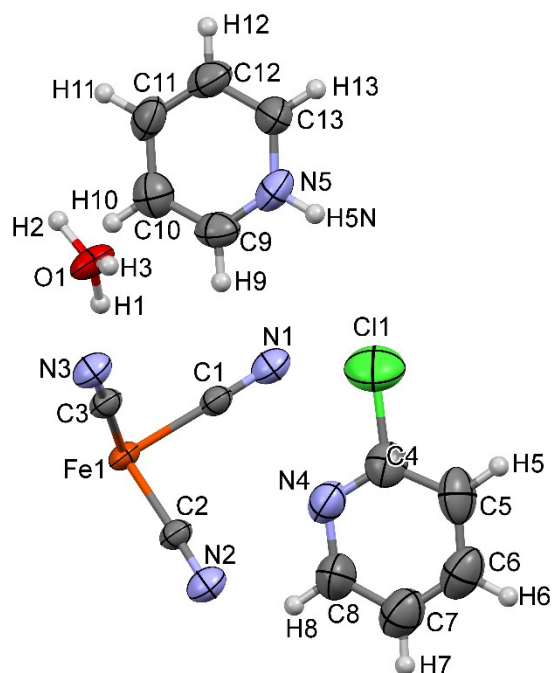|	V	VI	VII
Molecular formula	$C_{16}H_{16}Br_2FeN_8O_2$	$C_{16}H_{16}FeI_2N_8O_2$	$C_{18}H_{20}FeI_2N_8O_2$
M_r	568.00	662.00	690.1
Crystal system	monoclinic	monoclinic	monoclinic
Space group	$C\,2/c$	$C\,2/c$	$P\,2_1/c$
Crystal data:			
a / Å	14.7058(15)	14.9231(14)	8.8231(4)
b / Å	8.3867(6)	8.4115(7)	11.0729(3)
c / Å	18.3571(18)	18.7857(16)	13.2703(7)
α / °	90	90	90
β / °	108.439(11)	108.571(9)	106.027(5)
γ / °	90	90	90
V / Å^3	2147.81	2235.3	728.25(5)
Z	4	4	2
D_{calc} / g cm^{-3}	1.76	1.97	1.84
$\lambda(MoK_\alpha)$ / Å	0.71073	0.71073	0.71073
T / K	295	295	295
Crystal size / mm^3	0.32 x 0.29 x 0.26	0.35 x 0.30 x 0.25	0.34 x 0.25 x 0.16
μ / mm^{-1}	4.452	3.456	3.112
$F(000)$	1120	1264	664
Refl. collected/unique	7901 / 2302	6293 / 2422	7757 / 2680
Data/restraints/ parameters	145	145	140
$\Delta\rho_{max}$, $\Delta\rho_{min}$ / e Å^{-3}	0.66; −0.59	1.34;-1.43	0.75; −0.49
$R[F^2 > 4\sigma(F^2)]$	0.0309	0.0442	0.0301
$wR(F^2)$	0.072	0.112	0.064
Goodness-of-fit, S	1.075	1.036	0.872

Figure S1. Ortep plot of the asymmetric unit of **I** showing the atom-labelling scheme. Displacement ellipsoids are drawn at the 50 % probability level, and H atoms are shown as small spheres of arbitrary radius.
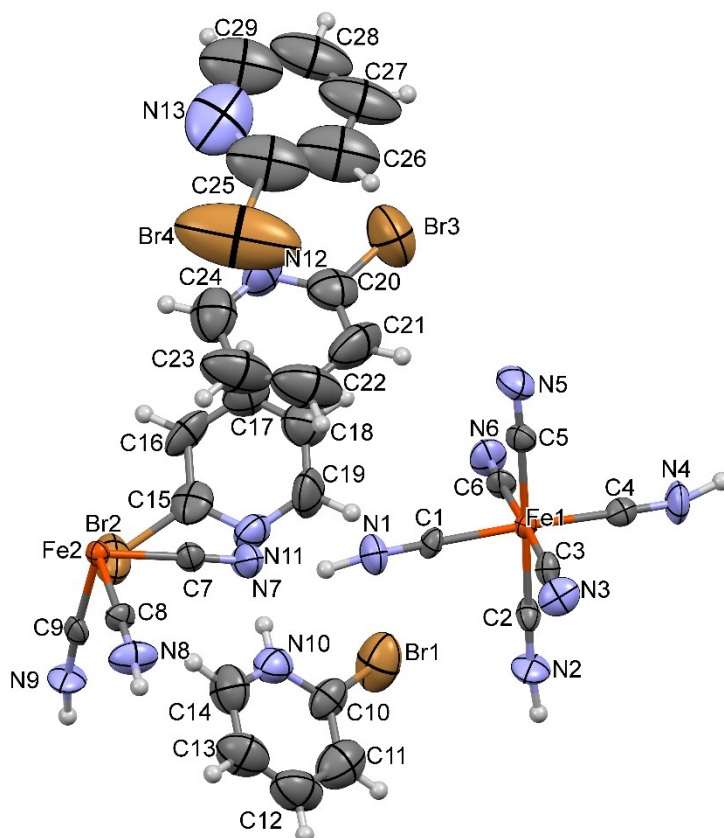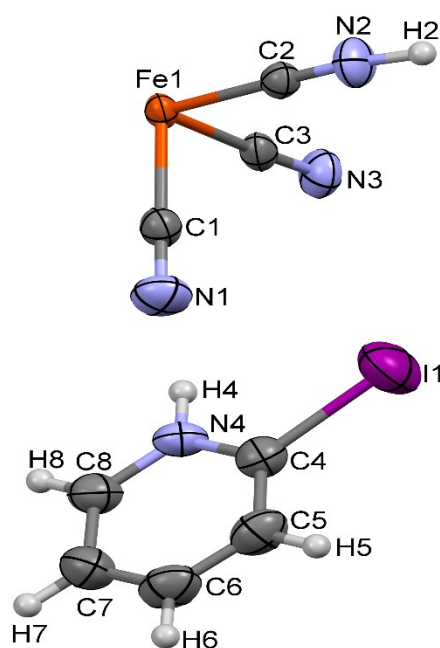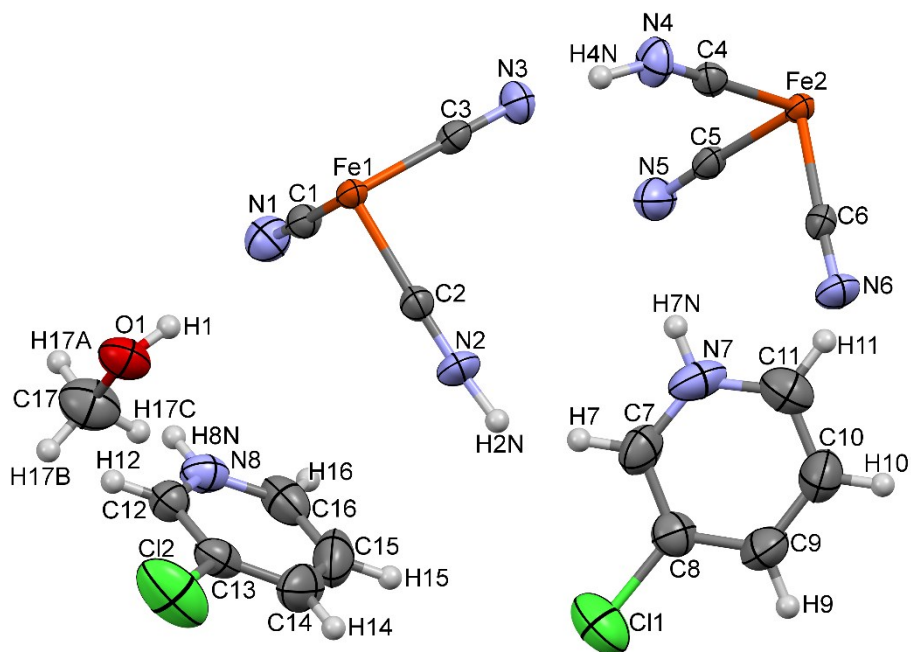

Figure S2. Ortep plot of the asymmetric unit of **II** showing the atom-labelling scheme. Displacement ellipsoids are drawn at the 50 % probability level, and H atoms are shown as small spheres of arbitrary radius.
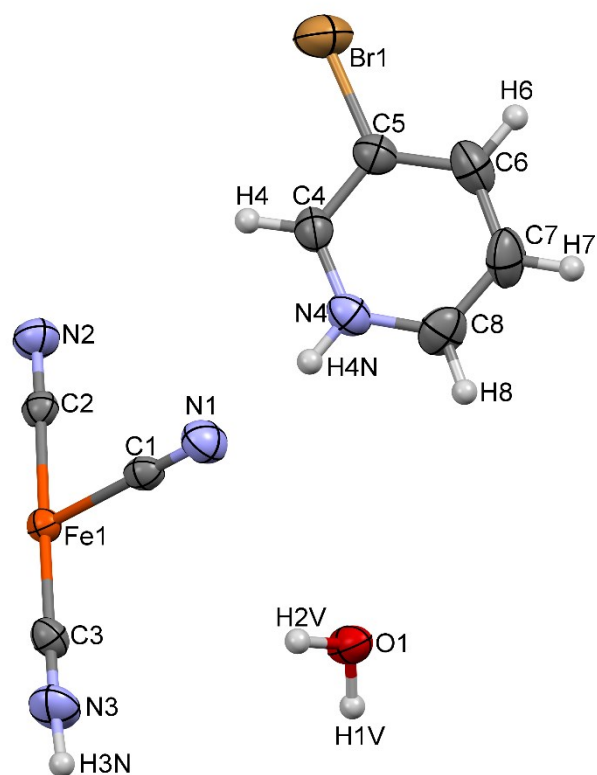
Figure S3. Ortep plot of the asymmetric unit of **III** showing the atom-labelling scheme. Displacement ellipsoids are drawn at the 50 % probability level, and H atoms are shown as small spheres of arbitrary radius.

Figure S4. Ortep plot of the asymmetric unit of **IV** showing the atom-labelling scheme. Displacement ellipsoids are drawn at the 50 % probability level, and H atoms are shown as small spheres of arbitrary radius.
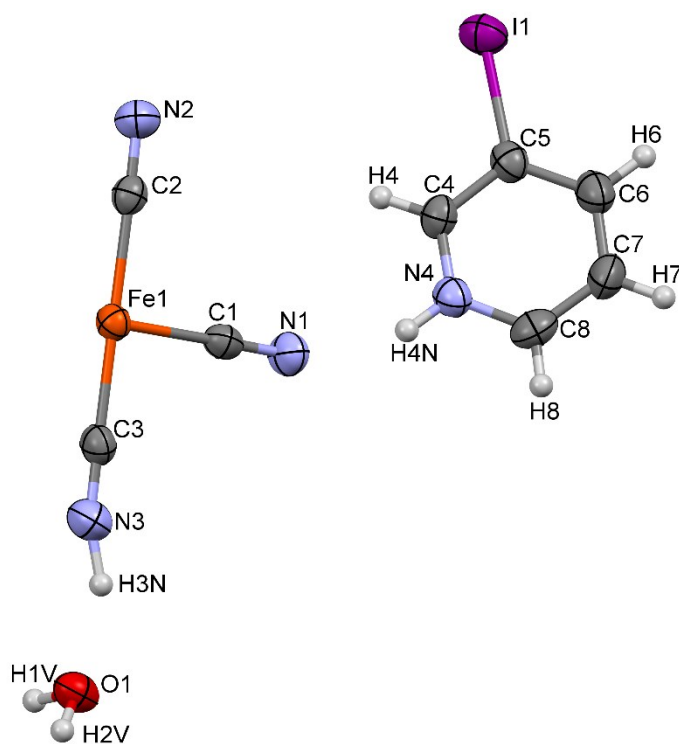
Figure S5. Ortep plot of the asymmetric unit of **V** showing the atom-labelling scheme. Displacement ellipsoids are drawn at the 50 % probability level, and H atoms are shown as small spheres of arbitrary radius.
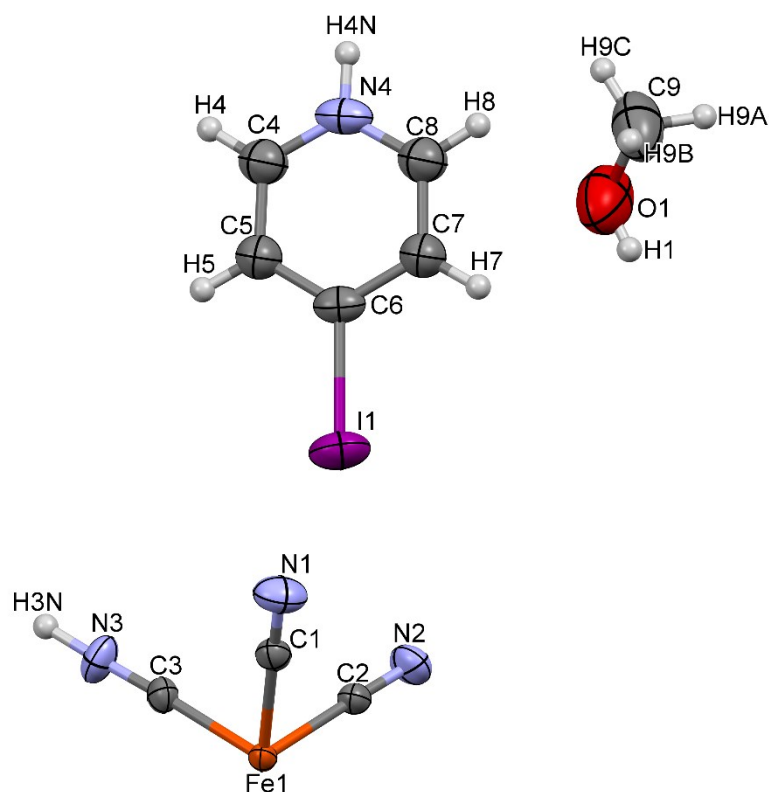

Figure S6. Ortep plot of the asymmetric unit of **VI** showing the atom-labelling scheme. Displacement ellipsoids are drawn at the 50 % probability level, and H atoms are shown as small spheres of arbitrary radius.

Figure S7. Ortep plot of the asymmetric unit of **VII** showing the atom-labelling scheme. Displacement ellipsoids are drawn at the 50 % probability level, and H atoms are shown as small spheres of arbitrary radius.

X-ray structural analysis

Diffraction measurements were made on an Oxford Diffraction Xcalibur Kappa CCD X-ray diffractometer with graphite-monochromated Mo $K\alpha$ (λ = 0.71073 Å) radiation.[17] The data sets were collected using the ω-scan mode over a 2ϑ range up to 54°. The structures were solved by SHELXT or by direct methods using the SHELXS and refined using SHELXL programs.[18] The structural refinement was performed on F^2 using all data. The hydrogen atoms not involved in hydrogen bonding were placed in calculated positions and treated as riding on their parent, while those involved in hydrogen bonding were located from the electron difference map whenever data quality was sufficient to render it possible. All calculations were performed, and the drawings were prepared using the WinGX crystallographic suite of programs.[19] Molecular structures of compounds are presented by ORTEP-3 [20] and their packing diagrams were prepared using Mercury.[21] The crystal data and measurement details are listed in Table S1. Further details are available in the Supporting Information and from the Cambridge Crystallographic Centre with quotation numbers 2031799-2031805.

A number of difficulties were encountered in the refinement of the structural models, mostly because of weak diffraction of the samples and because of the proton transfer between the hexacyanoferrate anions and water molecules or disordered solvent molecules placed in the voids of the hexacyanoferrate networks. It was therefore necessary to introduce multiple

restraints of bond distances and angles as well as thermal parameters in these parts of the structures.

In **I**, all the H_3O^+ protons were located from the electron difference map. The position of the proton in the [**2-Clpy**···H···**py**]$^+$ cation could not be reliably located from the electron difference map, and was located on the pyridine molecule according to the respective pK_a values of 2-chloropyridine and pyridine (0.49 and 5.14 in water at 25 °C respectively [22]). In **II**, the H3 proton is located close, but not quite exactly on the 2-fold axis and was modelled as disordered about the twofold axis with identical occupancy (0.50) for both positions. The remaining hexacyanoferrate hydrogen atoms were located from the electron difference map with several restraints of bond distances and angles according to the geometry of the molecules. The hydrogen atom within the [**2-Brpy**···H···**2-Brpy**]$^+$ two-molecular cations was located from the electron difference map and isotropically refined. To offset the charge of the anions of the remaining two symmetrically independent **2-Brpy** molecules must also be protonated, albeit with 50% probability. As one of the two symmetrically independent **2-Brpy** molecules is obviously an acceptor of a C-H···N hydrogen bond, the required 0.5 hydrogen atom was placed on the other. This molecule is severely disordered (probably due to this partial protonation), and locating the proton from the electron difference map was not possible, rather it was modelled as riding on the parent nitrogen. The modelling of the disorder also required multiple restraints of bond distances and angles as well as thermal parameters. In **IV** no reasonable positions of hydrogen atoms could be deduced from the electron difference map and all the hydrogen atoms were modelled as riding on parent nitrogen atoms. In the case of hydrogen bonded protonated cyanide nitrogen, the hydrogen position was modelled as disordered over two positions. In both **V** and **VI** the water and $H_2[Fe(CN)_6]^{2-}$ hydrogen bonding atoms were located in the electron difference map, while the hydrogen atoms on **3-Brpy**H$^+$ and **3-Ipy**H$^+$ pyridine nitrogen were placed on calculated positions as riding on the parent nitrogen.
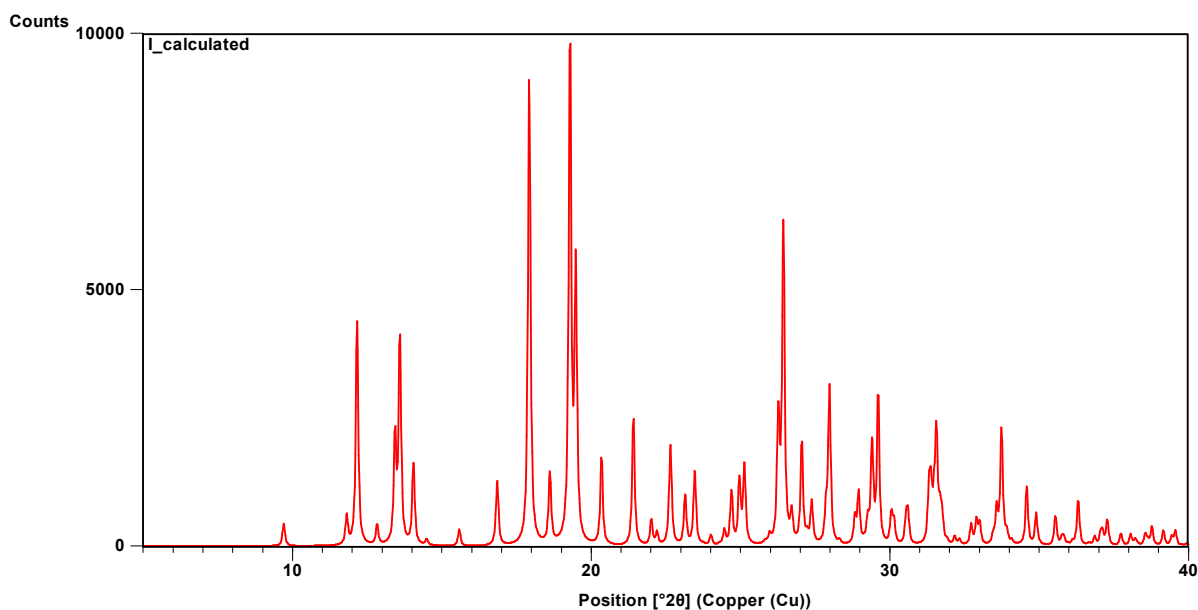

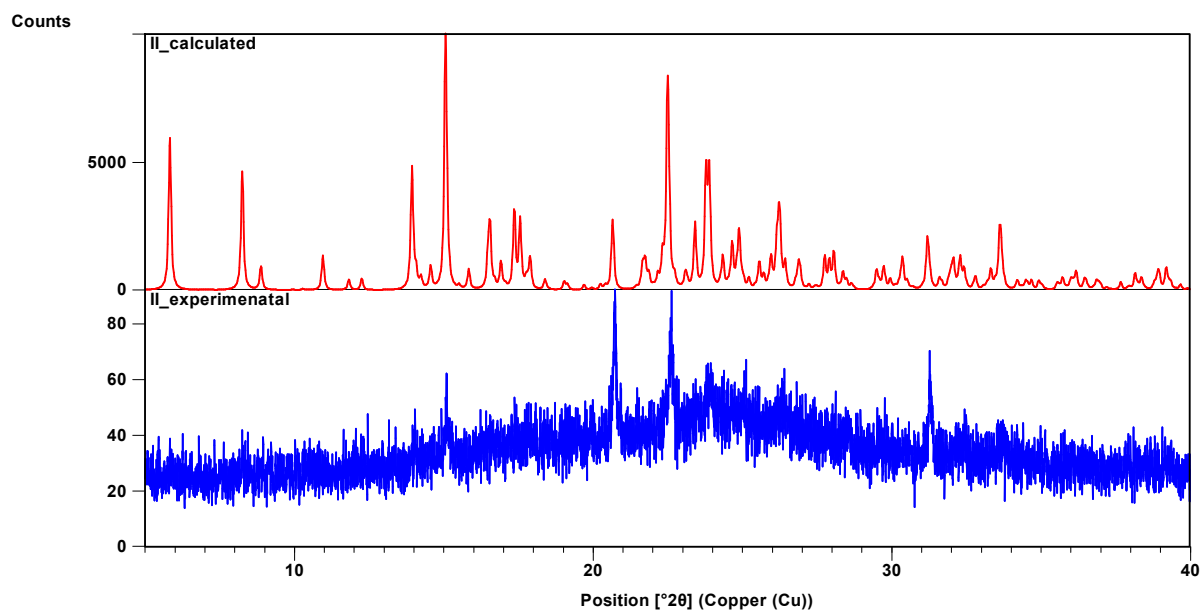Figure S8. Calculated XRPD patterns of **I**.

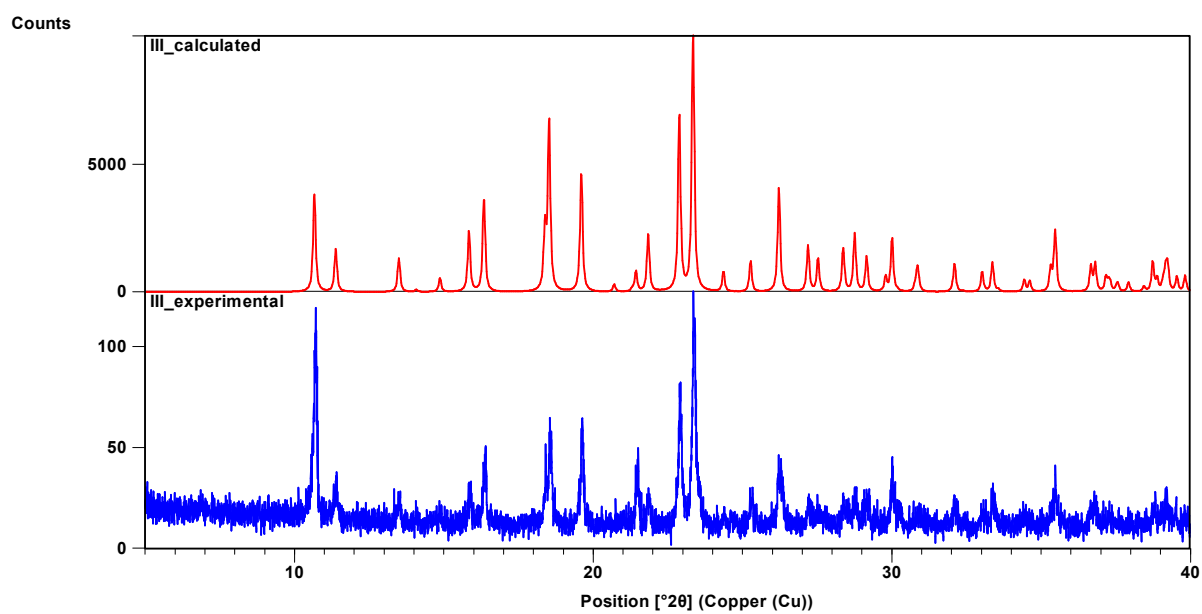Figure S9. Measured and calculated XRPD patterns of **II**.

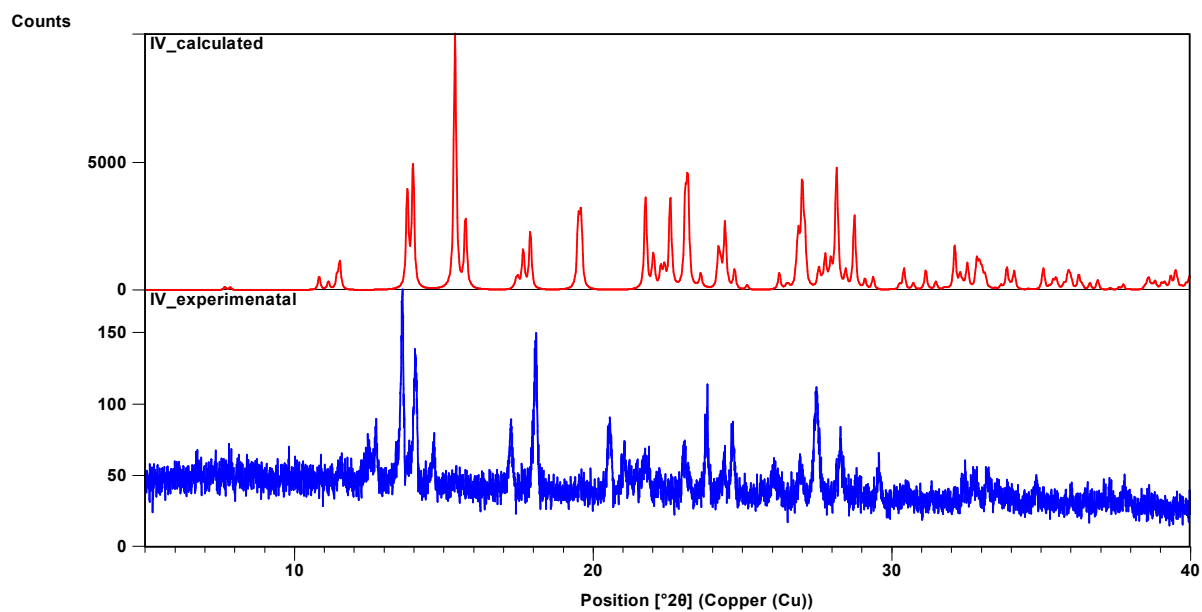Figure S10. Measured and calculated XRPD patterns of **III**.

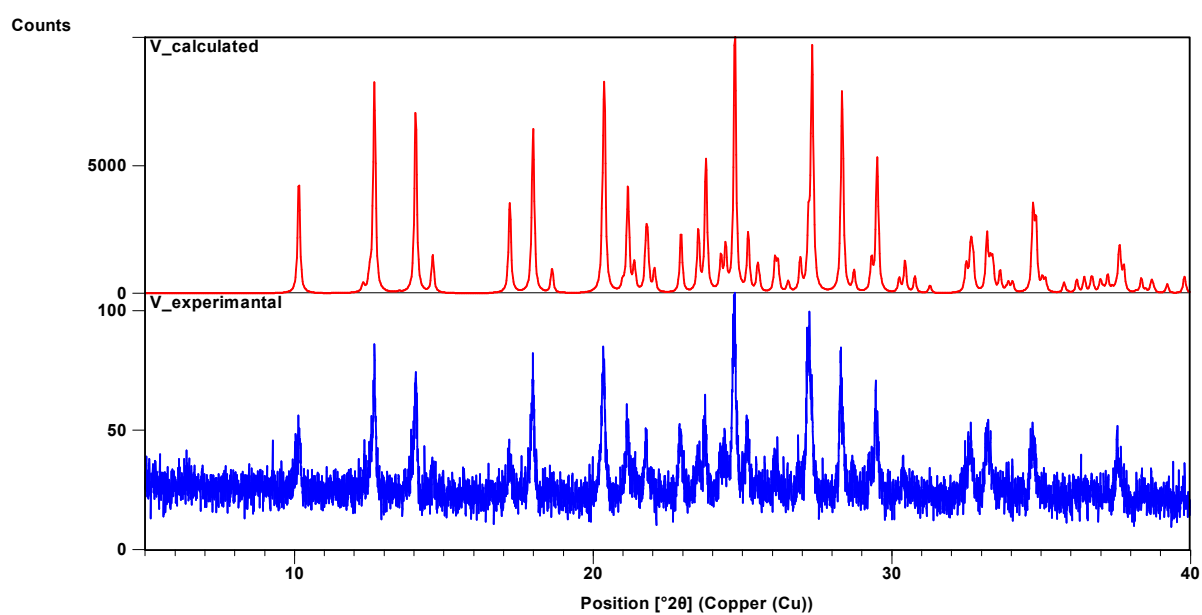Figure S11. Measured and calculated XRPD patterns of **IV**.

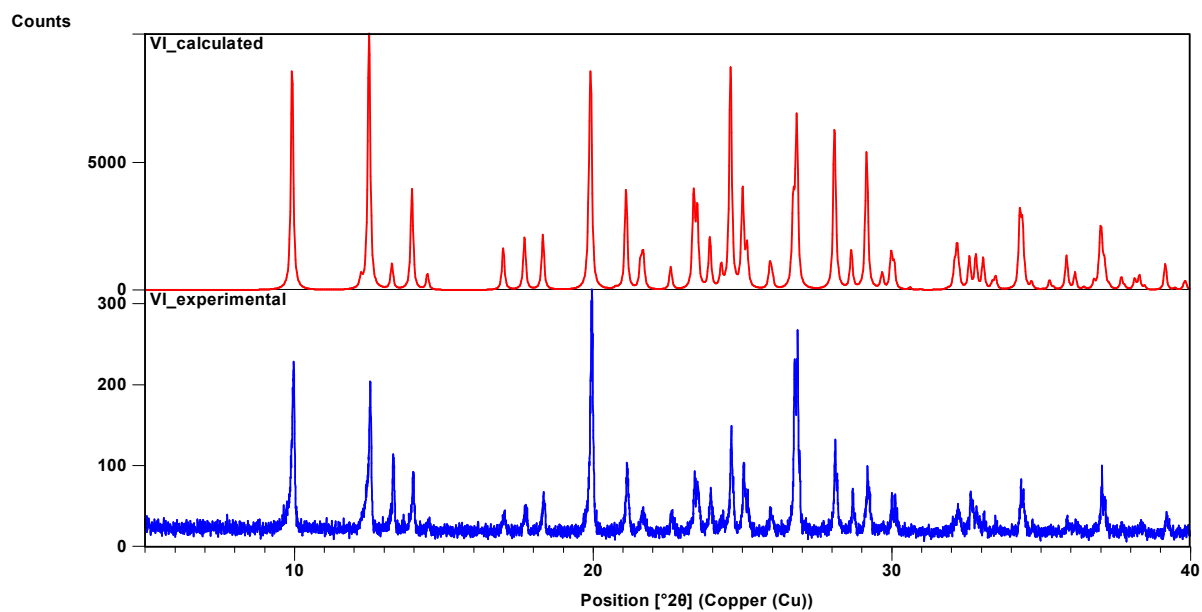Figure S12. Measured and calculated XRPD patterns of **V**.

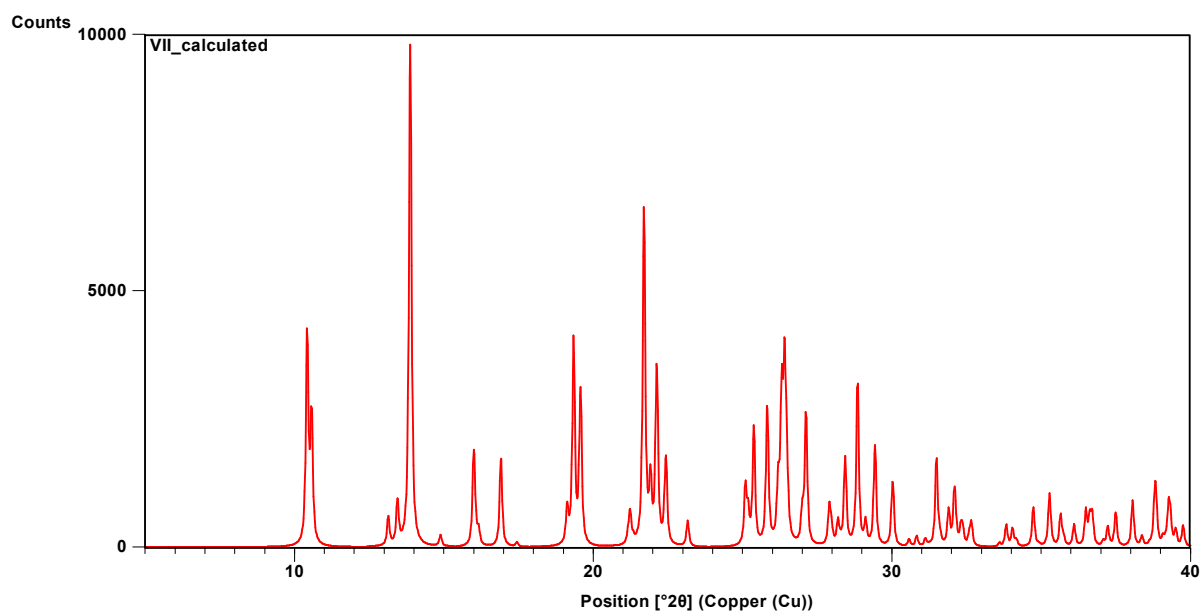Figure S13. Measured and calculated XRPD patterns of **VI**.
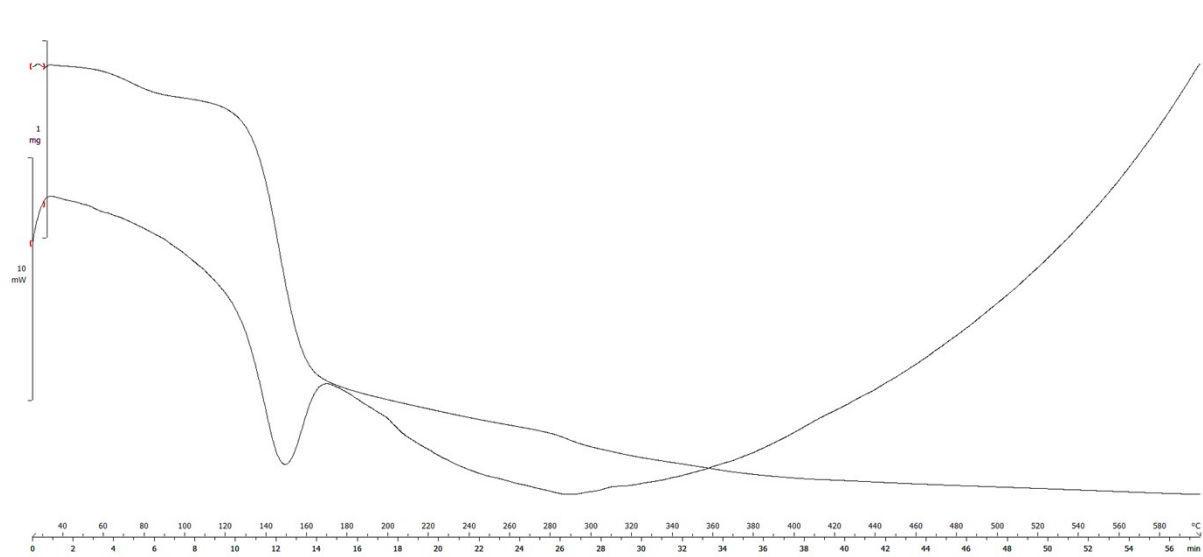

Figure S14. Calculated XRPD patterns of **VII**.

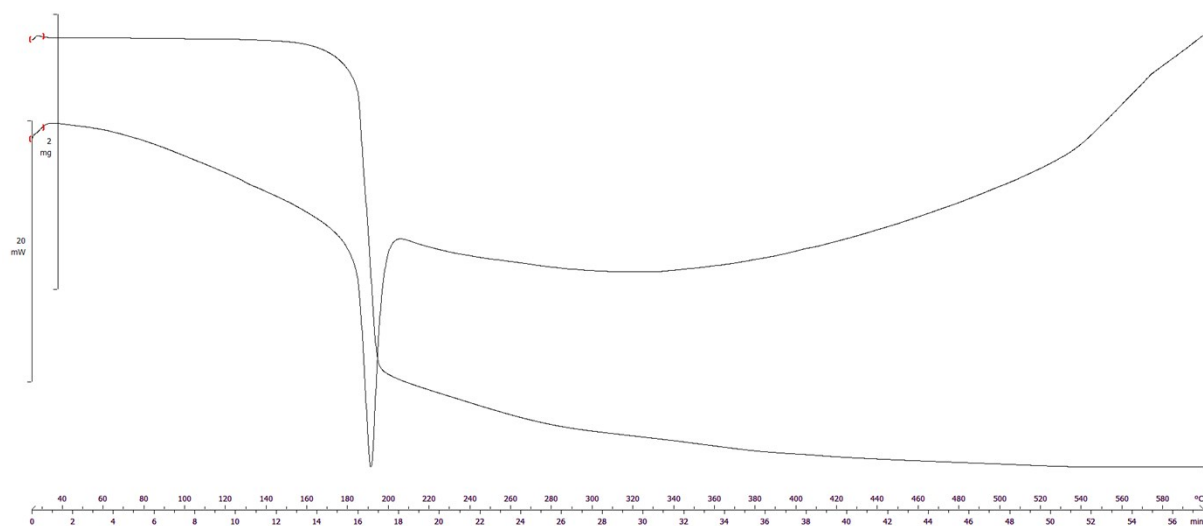Figure S15. DSC and TG thermogram of **II.**

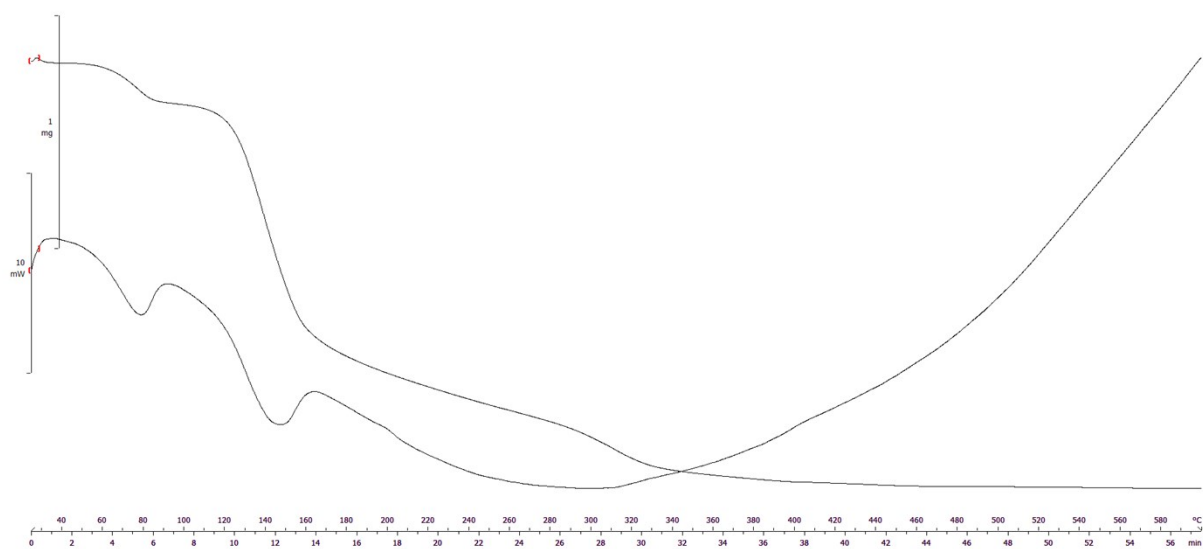Figure S16. DSC and TG thermogram of **III.**

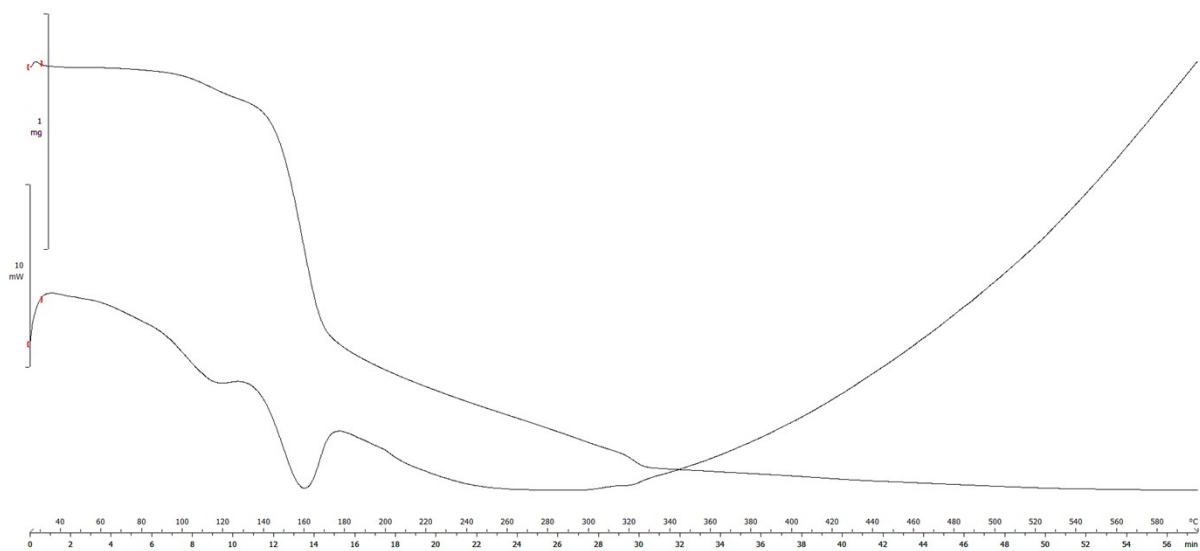Figure S17. DSC and TG thermogram of **V.**
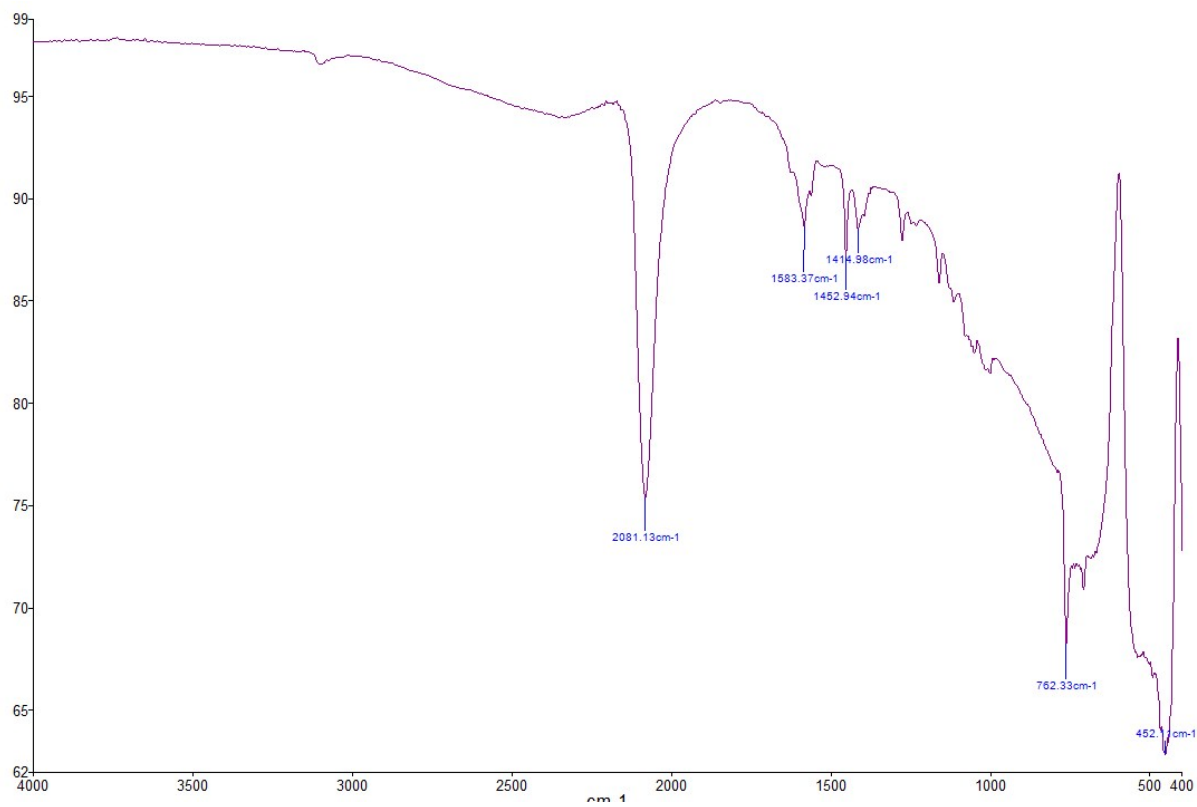

Figure S18. DSC and TG thermogram of **VI.**
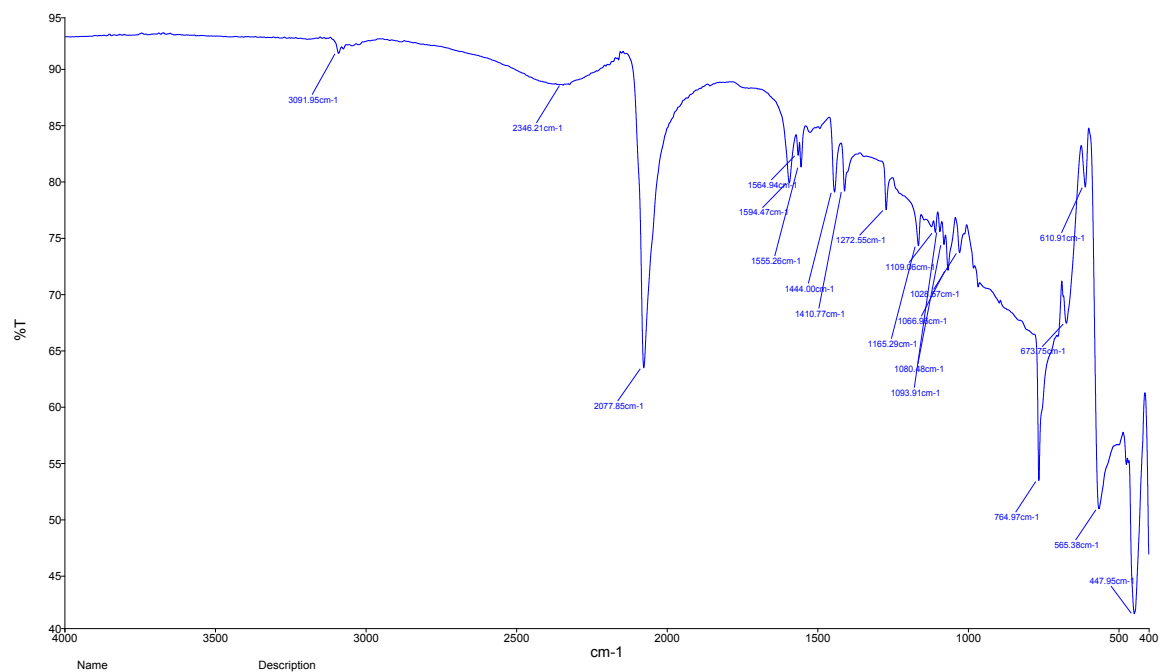
Figure S19. IR spectra of **II.**
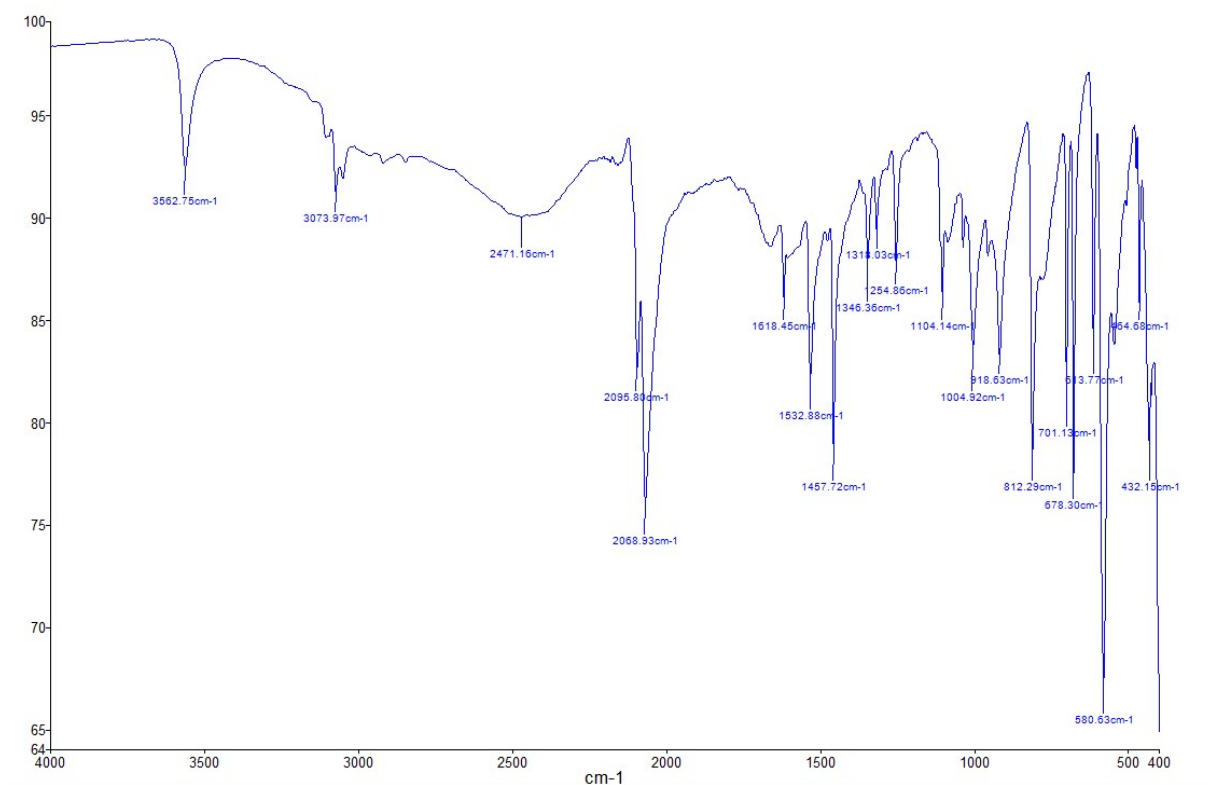

Figure S20. IR spectra of **III.**

14

Figure S21. IR spectra of **V.**

Figure S22. IR spectra of **VI.**

15

Table S2. Number of datasets in the CSD comprising protonated halogenopyridinium cation.

	Cl⁻	Br⁻	I⁻	O	N	other
2ClPy	4	2		2		
2BrPy	7	13	3			
2Ipy	2	4				
3ClPy	6	2	1	1		4
3BrPy	8	10	4	3		
3Ipy	7	5	1	1		
4ClPy	14	7	3	1		
4BrPy	12	9	3	2		1
4Ipy	4	2	1	3		1

References

1. Oxford Diffraction (2003), CrysAlis CCD and CrysAlis RED. Version 1.170., Oxford Diffraction Ltd, Wroclaw, Poland.
2. G. M. Sheldrick, *Acta Cryst.* 2008, **A64**, 112.
3. L. J. Farrugia, *J. Appl. Cryst.*, 1999, **32**, 837.
4. L. J. Farrugia, *J. Appl. Cryst.*, 1997, **30**, 565.
5. C. F. Macrae, I. J. Bruno, J. A. Chisholm, P. R. Edgington, P. McCabe, E. Pidcock, L. Rodriguez-Monge, R. Taylor, J. van de Streek and P. A. Wood, *J. Appl. Cryst*. 2008, **41,** 466.
6. R. H. Linnell, *J. Org. Chem.*, 1960, **25**, 290.
7. A. Gero and J. J. Markham, *J. Org. Chem.* 1951, 16, 12, 1835–1838.